Computer simulation of γ′ and θ phase precipitation of Ni‒Al‒V alloy using microscopic phase-field method [①]

LI Yong-sheng(李永胜) , CHEN Zheng(陈　铮) ,

WANG Yong-xin(王永欣) , Lu Yan-li(卢艳丽)

(School of Materials Science and Engineering,

Northwestern Polytechnical University, Xi'an 710072, China)

Abstract: The precipitation processes of γ′ and θ phases in $Ni_{75}Al_{6.5}V_{18.5}$ alloy were simulated at different temperatures and the precipitation sequence of two phases and morphological evolution were investigated. The simulation demonstrates that the two phases precipitate simultaneously at high temperature and γ′ phase precipitates earlier than θ phase at 1 000 K and 1 120 K. With the temperature decreasing, the velocity of precipitation quickens, the quantity of θ phase increases and the size reduces; but the volume fraction increases, the quantity of phase increases and the size reduces as well. The two phases nucleate and grow independently at high temperature and the θ phase precipitates from the boundaries of γ′ phase at 1 000 K and 1 120 K. We also find that there are many kinds of domain boundaries between the same and different phases. The results of average deviation of composition and average absolute long range order parameter show that the ordering and compositional clustering of γ′ phase happen simultaneously at high temperature, the congruent ordering occurs prior to spinodal decomposition at 1 000 K and 1 120 K and the ordering advances and quickens as the temperature decreases. Ordering and compositional clustering of θ phase occur simultaneously at each temperature and are quickened with temperature decreasing.

Key words: microscopic phase-field; precipitation; atomic configuration; ordering; spinodal decomposition; simulation

CLC number: TG 111. 5   **Document code: A**

---

1 INTRODUCTION

With the increasing demand on application of materials, computer simulation technique has an important effect on designing and exploiting new materials. Studying the real alloy systems with computer is significant to the industrial production. The precipitation behavior of alloys during ageing has an important effect on the properties of materials. Investigating the influencing factor of morphology during precipitation, searching the phenomena that are difficult to observe during the experiments and confirming the precipitation mechanisms are the basic conditions for optimizing alloy systems. Molecular dynamics[1], Monte Carlo[2] and phase-field method[3, 4] have been widely used on microscopic morphological studying of alloys. Khachaturyan proposed the microscopic lattice diffusion theory[5] and established the microscopic phase field kinetic model[6], which has been used successfully in the simulation of alloy precipitation process on atomic scale[7‒10].

Nickel-based intermetallics Ni_3X which have topological close packed structure, have their own characteristic properties as high temperature structure and chemical materials[11]. With the atomic configuration and order parameter, we investigated the morphological evolution at different temperatures and the effect of thermodynamic conditions on precipitation velocity and mechanism of pseudo-binary Ni_3Al‒Ni_3V system firstly. There were two phases precipitation at the composition that was studied, which were γ′ and θ[12, 13]. We simulated the state of 1 250 K, 1 120 K and 1 000 K, which were above the $L1_2$ and DO_{22} instability lines, between the $L1_2$ and DO_{22} instability lines and below the DO_{22} instability line on the diagram that was proposed by Poduri and Chen[14].

2 MICROSCOPIC PHASE-FIELD MODEL

The process of precipitation is nonequilibrium and nonlinear, which can be described by the Onsager-type microscopic diffusion equation that was proposed by Khachaturyan[5]. The equation has been used in the simulation of precipitation of binary alloy systems. In this model, the atomic configurations and morphologies are described by single-site occupation probability functions $P_A(r, t)$, $P_B(r, t)$, $P_C(r, t)$, which represent the probability of finding an A, B or C atom at a given lattice site and at a given time t. For ternary system,

---

$P_A(r, t) + P_B(r, t) + P_C(r, t) = 1$, and only two equations are independent at each lattice site, so we can get the microscopic diffusion equation of ternary system[15]. In order to describe the nucleation, we add a random noise item to the right-hand side of the equation, so we have the microscopic Langevein equation:

$$\frac{dP_A(r, t)}{dt} = \frac{1}{k_B T} \sum_{r'} \left[L_{AA}(r - r') \frac{\partial F}{\partial P_A(r', t)} + \right.$$
$$\left. L_{AB}(r - r') \frac{\partial F}{\partial P_B(r', t)} \right] + \xi(r, t) \qquad (1a)$$

$$\frac{dP_B(r, t)}{dt} = \frac{1}{k_B T} \sum_{r'} \left[L_{BA}(r - r') \frac{\partial F}{\partial P_A(r', t)} + \right.$$
$$\left. L_{BB}(r - r') \frac{\partial F}{\partial P_B(r', t)} \right] + \xi(r, t) \qquad (1b)$$

where $L(r - r')$ is a constant related to the exchange probabilities of a pair of atoms, α and β, at lattice site site r and r' per unit time; α, $\beta = A$, B or C. F is the total free energy of the system.

$\xi(r, t)$ is assumed to be Gaussian-distributed with the average value of zero, which is uncorrelated with space and time. It obeys the so-called fluctuation dissipation theory[16]:

$$\langle \xi(r, t) \rangle = 0 \qquad (2a)$$
$$\langle \xi(r, t) \xi(r', t') \rangle = - 2k_B T L(r - r') \cdot$$
$$\delta(t - t') \delta(r - r') \qquad (2b)$$

where $\langle ... \rangle$ denotes an average, $\langle \xi(r, t) \rangle$ is the average value of the thermal fluctuation over space and time; $\langle \xi(r, t) \xi(r', t') \rangle$ is the correlation and δ is the Kronecker delta function.

Based on mean-field approximation, F is given by the following equation:

$$F = - \frac{1}{2} \sum_r \sum_{r'} [V_{AB}(r - r') P_A(r) P_B(r') +$$
$$V_{BC}(r - r') P_B(r) P_C(r') +$$
$$V_{AC}(r - r') P_A(r) P_C(r')] +$$
$$k_B T \sum_r [P_A(r) \ln(P_A(r)) +$$
$$P_B(r) \ln(P_B(r)) + P_C(r) \ln(P_c(r))] \qquad (3)$$

where $V_{\alpha\beta}(r - r')$ is the interaction energy between α and $\beta (= A$, B or C) at the lattice site of r and r'.

It will simplify the solution process by taking Fourier transformation of Equation (1), solving it in the reciprocal space, and transforming it into the real space, i. e. transforming a 3-D nonlinear question into a 2-D linear one. We can obtain the intuitionistic atomic configuration through this method and describe the phase structure and morphology of the precipitation process.

3 SIMULATION RESULTS AND DISCUSSION

3. 1 Precipitation process at high temperature

The degree of undercooling of system is relatively low at high temperature, and it's difficult to nucleate, so that it needs to add certain thermal fluctuations in the simulation. The thermal fluctuations are 3 000 time-steps. The γ' and θ phases nucleate simultaneously at this temperature, but the size of γ' phase is larger than that of θ phase, as shown in Fig. 1(b), in which both $L1_2$ and DO_{22} structures exist. The thermal fluctuations are just removed in Fig. 1(a) and the system is in critical state, so many ordered phase embryos appear. In the simulation processes, some embryos of θ phase disappear, which are labeled with arrows in Figs. 1(a), (b) and (c). This demonstrates that these embryos can't become critical nuclei. But the other embryos remain and grow into steady nucleus and then become ordered phases. We can see that the size of the disappeared embryos are not smaller than those remained and some are even larger than those remained. Our study is consistent with the critical nucleus of $\delta'(Al_3Li)$ phase studied by LI et al[17]. But the γ' phase dose not have this phenomenon. In order to show the nucleation of γ' phase, we give the atomic evolution configuration at initial state (Fig. 2). The reason for this phenomenon is that the alloy is close to $L1_2$ instability line but far from DO_{22} instability line, and the driving force of the precipitation of γ' phase is larger than that of θ phase at this content and temperature. It can be seen from the atomic evolution configuration that the nucleation and growth rate of γ' phase is higher and the size is larger than that of θ phase. The shape of both phases transforms from equiaxial to massive as shown in Figs. 1(c) and (d).

It can be seen that at $t = 100\,000$ time-steps, the two phases or the same phases combine each other. Three kinds of homophase boundaries among γ' phases form, as shown in Fig. 3, which are labeled with arrows A, B and C; there are five kinds of heterophase boundaries between γ' phase and θ phase, which are labeled with D, E, F in [01] direction of the projection of DO_{22} and G, H in [10] direction of DO_{22}.

Figs. 4 (a) and (b) show the variation of average absolute deviation of the local composition from the overall average composition and average absolute value of long range order parameters. Both curves increase quickly and attain a value and then fall initially, which is due to the withdrawal of thermal fluctuations. Then the deviation of composition and average long range order parameter increase simultaneously, which demonstrates that ordering and compositional clustering take place at the same time. So we consider that there isn't GP zone before the precipitation of γ' and θ phases at high temperature, i. e. above the $L1_2$ and DO_{22} instability lines. It is also found that there isn't GP zone before the precipitation of δ' phase in
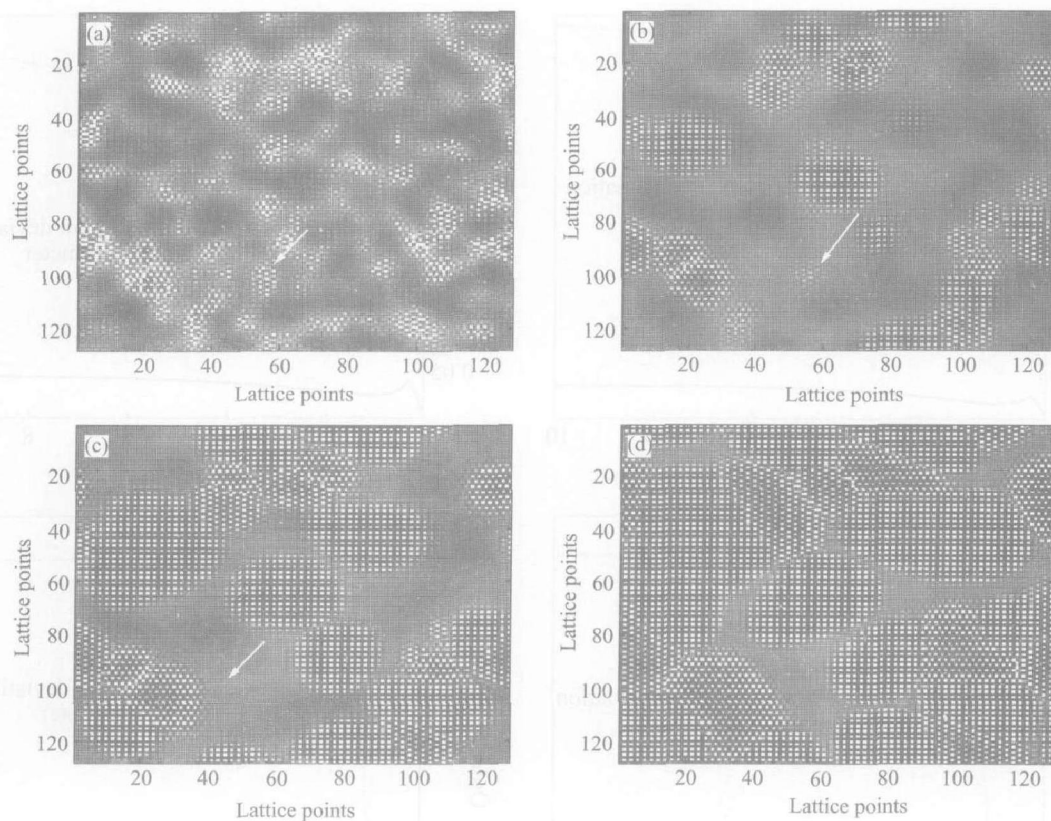
Fig. 1　Temporal evolution of occupation probabilities of $Ni_{75}Al_{6.5}V_{18.5}$ alloy at 1 250 K
(a) —t= 4 000; (b) —t= 10 000; (c) —t= 20 000; (d) —t= 100 000
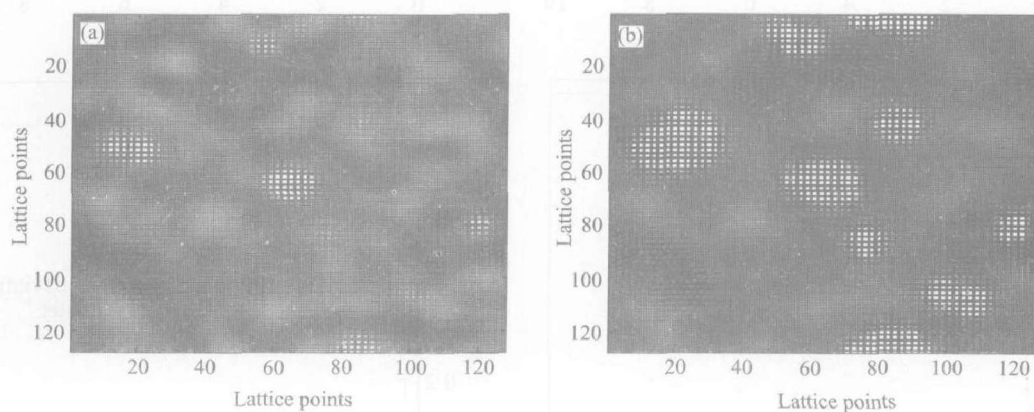

Fig. 2　Temporal evolution of occupation probabilities of $\acute{\gamma}$ phase at 1 250 K
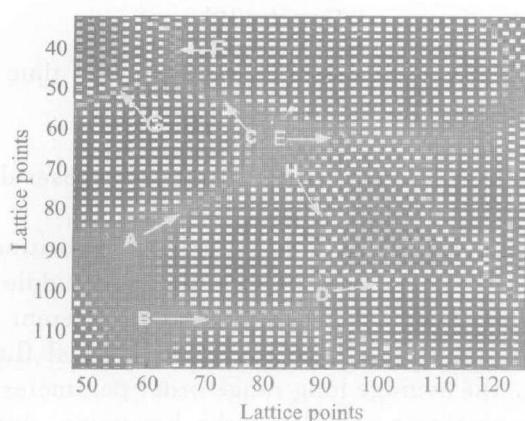(a) —t= 6 000; (b) —t= 12 000

Fig. 3　Domain boundary structure of
$Ni_{75}Al_{6.5}V_{18.5}$ alloy at 1 250 K(t= 100 000)

the metastable region of Al_3Li phase by LI[18].

3. 2　Precipitation process at middle temperature

It can be seen from the atomic evolution configuration that the $\acute{\gamma}$ phase precipitates firstly at this temperature, as shown in Fig. 5(a). The critical nucleus of $\acute{\gamma}$ phase grows steadily and forms ordered phase as time goes by. Then domain boundaries form among the massive ordered phases (Fig. 5(b)). The V atoms begin to precipitate around the domain boundaries which have the structure characteristic of DO_{22}, and occupy the positions of Al atoms. So the θ phases nucleate along the horizontal and vertical directions and form the
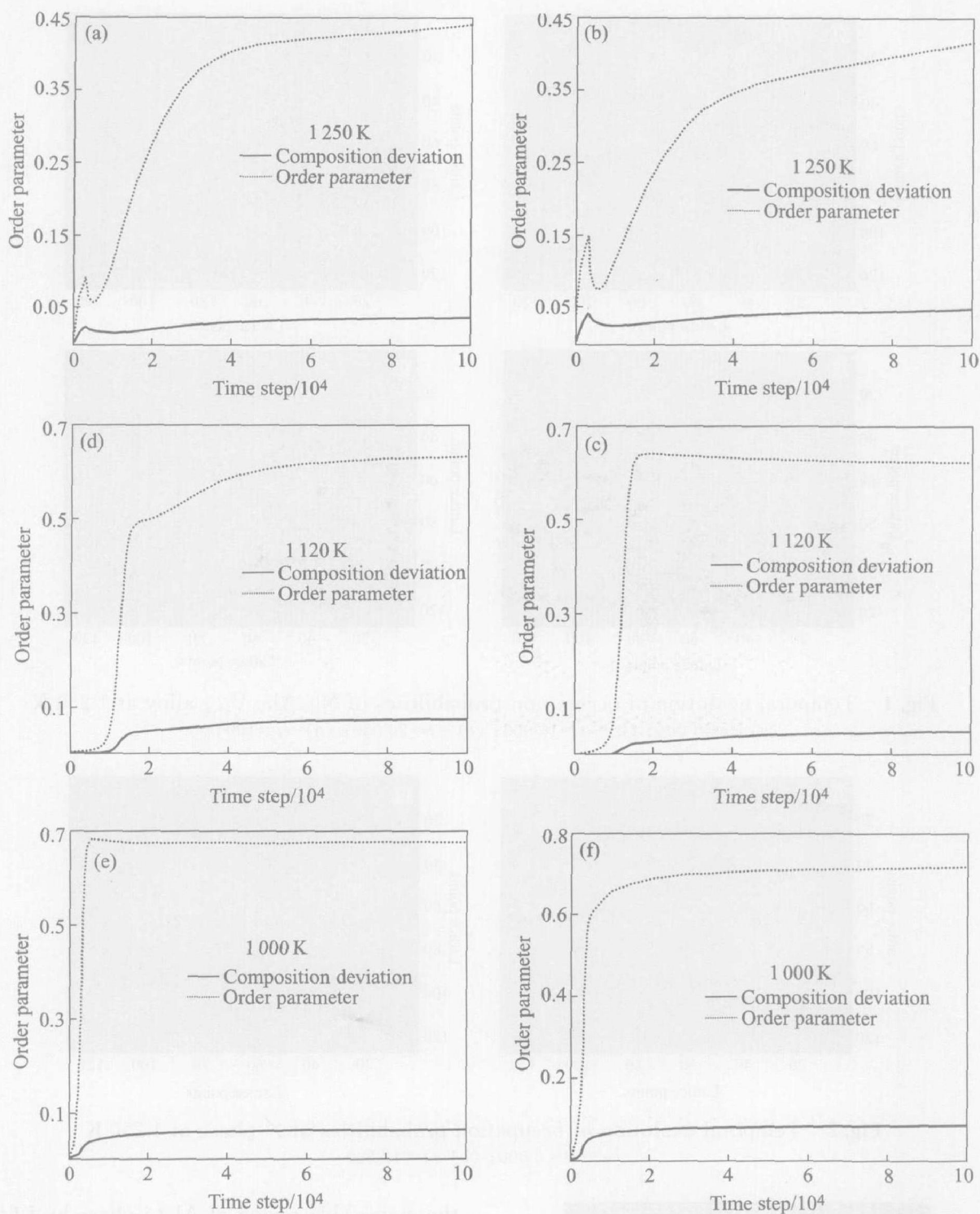
Fig. 4   Variation of deviation of composition and average long range order parameter with time
(a), (c), (e) —γ' phase; (b), (d), (f) —θ phase

strip shape (Fig. 5(c)). Then θ phases grow along the domain boundaries and the perpendicular direction of γ' phases. Finally the θ phases combine partially and the γ' phase are segregated. The size of γ' phases decreases as the phases become large. For the phases θ precipitated around the domain boundaries instead of nucleation from disordered matrix, there aren't the boundaries of G and H of Fig. 3 and the most boundaries are the same as D, E, F of Fig. 3, as shown in Fig. 5(d). The new homophase boundaries form among θ phases due to

the combination of phases.

The variations of deviation of composition and average long range order parameter at middle temperature (Fig. 4(c) and (d)) are different from that of 1 250 K. Since there are thermal fluctuations, the average long range order parameter of γ' phase increases quickly at the beginning, but the deviation of composition remains almost zero and begins to increase when the average long range order parameter attains the maximum. This stage corresponds to congruent ordering. Then the aver-
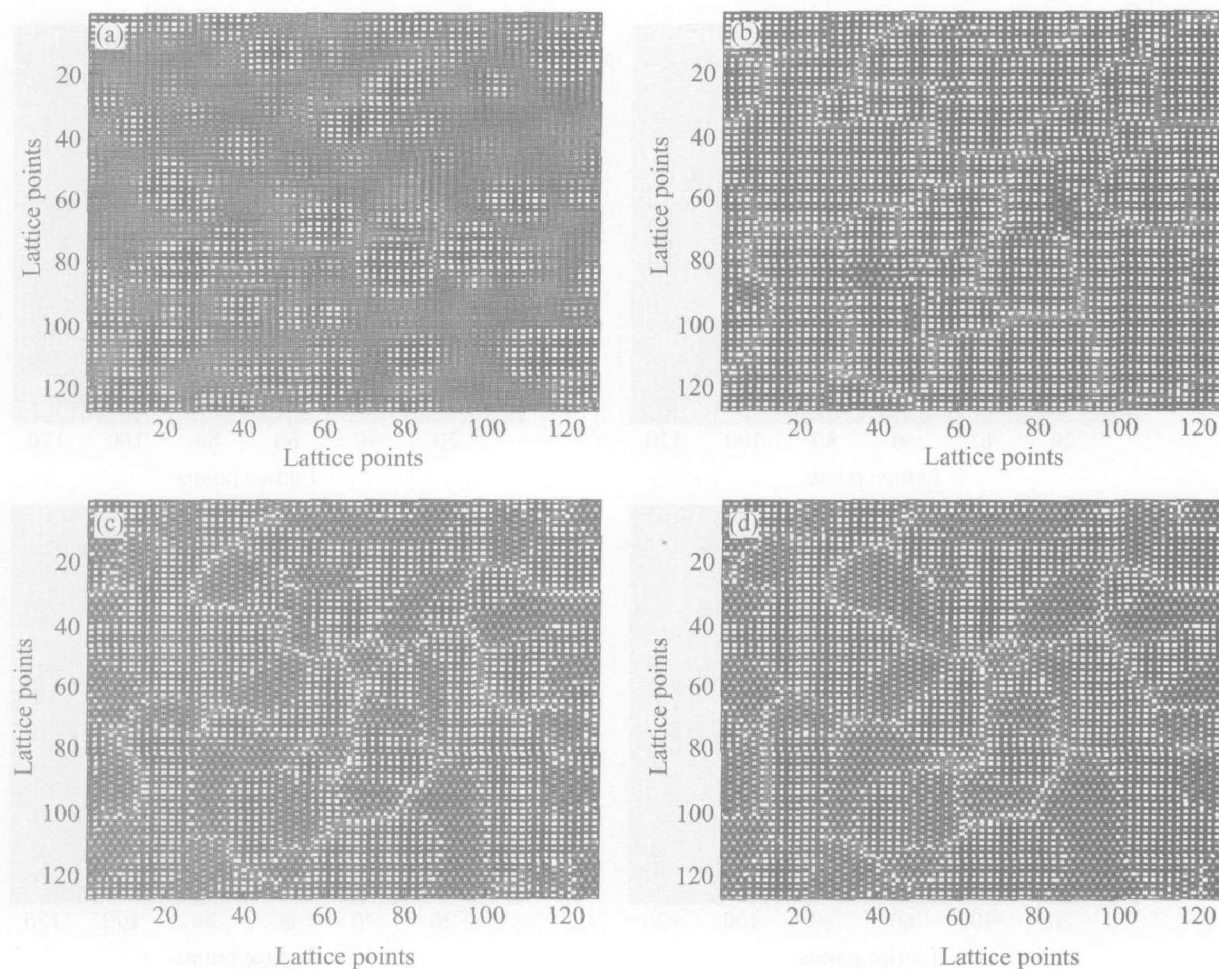
Fig. 5   Temporal evolution of occupation probabilities of $Ni_{75}Al_{6.5}V_{18.5}$ alloy at 1 120 K
(a) —t= 6 000; (b) —t= 12 000; (c) —t= 40 000; (d) —t= 100 000

age long range order parameter begins to fall and the deviation of composition increases quickly and then slowly, which is consistent with the spinodal decomposition. So the congruent ordering occurs prior to the spinodal decomposition at this temperature, for the ordering needs only short range diffusion but the spinodal decomposition needs long range diffusion. Pareige et al[19] also found that $L1_2$ ordered zones appeared before the decomposition. The variations of the deviation of composition and average long range order parameter of θ phase increase almost simultaneously and the average long range order parameter doesn't fall after it attains the maximum, so the ordering and compositional clustering happen simultaneously but are faster than those of 1 250 K.

3.3   Precipitation process at lower temperature

Fig. 6(a) shows the atomic configuration at t= 3 000 time-steps. We can see the nucleus of γ' phases and the V atoms in the map simulated, but the θ phases don't form at this time. As the simulation processes, the γ' phases nucleate and grow into ordered phases and the size is smaller than that of 1 120 K. From the time-steps and configu-

ration of ordered phase, it can be seen that the velocity of precipitation is twice as large as that of 1 120 K. Neither the θ phase nucleate and grow independently as that of 1 250 K, nor precipitation around the domain boundaries forms by γ' phase, but precipitate from the boundaries and corners of γ' phases forms as γ' phases growing. Parts of θ phases amalgamate or combine each other as the growth processes and some small γ' phases are swallowed up by θ phases as well as some small θ phases. Two phases are coarsened by the migration of boundaries and form the domain boundaries just as 1 120 K.

Comparing the variations of deviation of composition and average long range order parameter (Fig. 4(e), (f)) with that of 1 120 K, it can be seen that the velocity of ordering of γ' phases advances and quickens at lower temperature. The spinodal decomposition begins when the average long range order parameter increases to a certain value. The variations of the deviation of composition and average long range order parameter of phases are similar but quicker than those of 1 120 K.

3.4   Comparison with correlation experiment

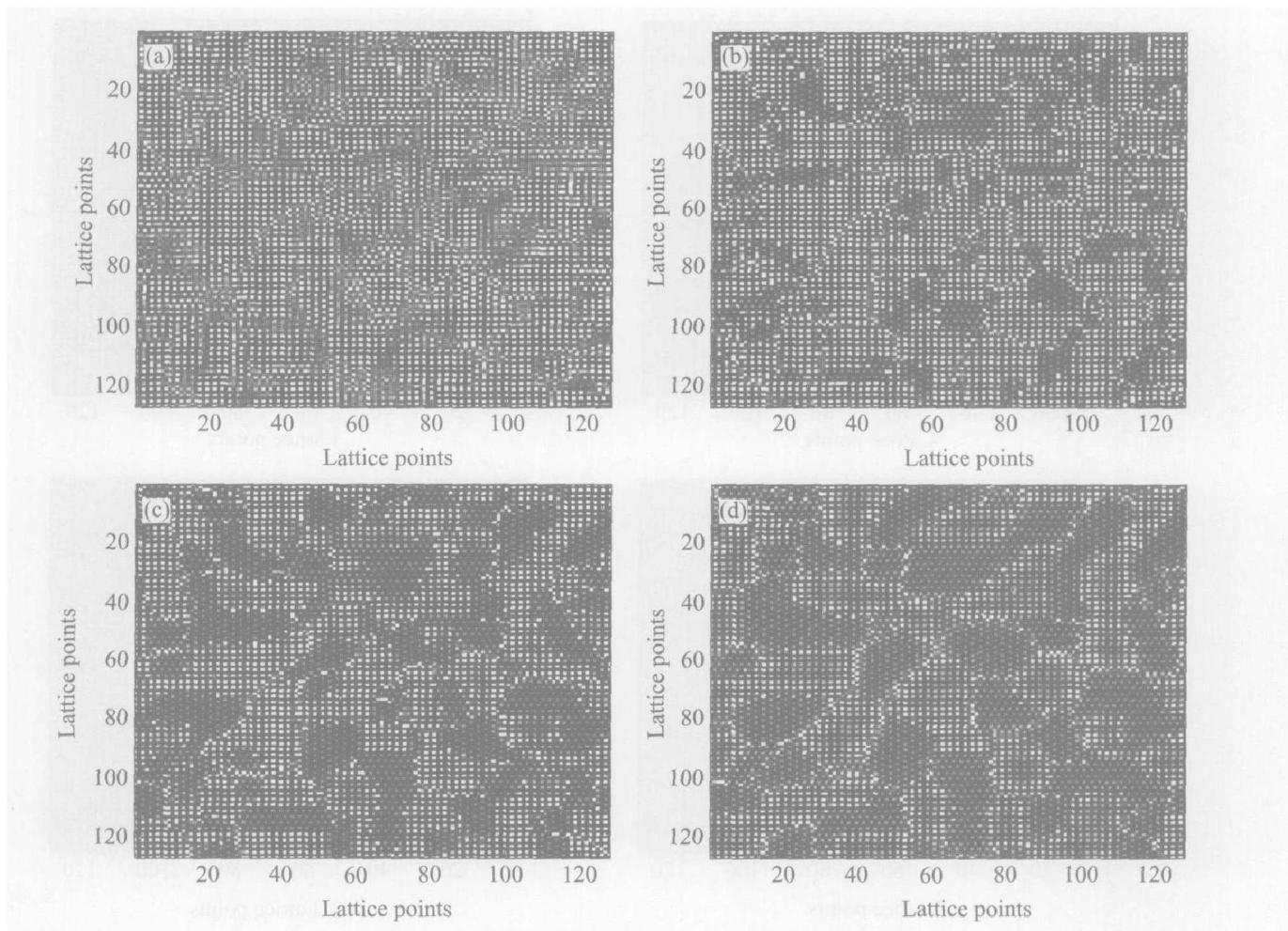Bendersky et al[20]   studied   the   precipitation

Fig. 6　Temporal evolution of occupation probabilities of $Ni_{75}Al_{6.5}V_{18.5}$ alloy at 1 000 K
(a) —t= 3 000; (b) —t= 6 000; (c) —t= 20 000; (d) —t= 100 000

process of Ni-Al-V alloys with TEM and X-ray diffraction, and demonstrated the precipitation order and transformation path of γ' and θ phases. Zapolsky et al[12] studied the precipitation order of γ' and θ phases of $Ni_{78.5}Al_7V_{14.5}$ alloy with the 3DAP technique, which showed that the two phases precipitated simultaneously at 800 ℃. The precipitation process predicted from our simulation agrees with the experimental observations, and the ordering and compositional clustering, critical nucleus will be clarified further.

4　CONCLUSIONS

1) The γ' and θ phases precipitate simultaneously at high temperature and γ' phase precipitates earlier than θ phase at 1 000 K and 1 120 K. With the temperature decreasing, the velocity of precipitation of two phases is quickened, the quantity of θ phase increases and the size reduces but the volume fraction increases, the quantity of γ' phase increases and size reduces as well.

2) There are the phenomena of disappearance of γ' phase critical nucleus at high temperature but the critical nucleus grows steadily at 1 000 K and 1 120 K. This indicates that the driving force for precipitation increases as temperature falls. The domain boundaries

are more at high temperature than those at 1 000 K and 1 120 K as the two phases nucleate and grow independently at high temperature.

3) Ordering and compositional clustering of γ' phase happen simultaneously at high temperature and the congruent ordering is prior to spinodal decomposition at middle and lower temperatures. With the temperature decreasing, the ordering is advanced and quickened. Ordering and compositional clustering of θ phase occur simultaneously at each temperature and is quickened with temperature decreasing.

REFERENCES

[1]　Liu H B, Canizal G, Jiménez S, et al. Molecular dynamics simulation on edge dislocation in the bulk and nanoparticles of iron [J]. Computational Materials Science, 2003, 27: 333 - 341.

[2]　Gotoa K, Saitoa Y, Suwa Y. Monte Carlo simulation of phase separation in iron-based ternary alloys [J]. Intermetallics, 2003, 11: 1267 - 1272.

[3]　Simmons J P, Wen Y H, Shen C, et al. Microstructural development involving nucleation and growth phenomena simulated with the phase field method [J]. Materials Science and Engineering, 2004, A365: 136 - 143.

[4]　Shen C, Chen Q, Wen Y H, et al. Increasing length scale of quantitative phase field modeling of concurrent

growth and coarsening processes [J]. Scripta Materialia, 2004, 50: 1029 ~ 1034.

[5]　Khachaturyan A G. Theory of Structural Transformation in Solids [M]. New York: Wiley, 1983. 129 ~ 136.

[6]　Chen L Q, Khachaturyan A G. Computer simulation of structural transformations during precipitation of an ordered intermetallic phase [J]. Acta Metall Mater, 1991, 39(11): 2533 ~ 2551.

[7]　LI Xiao-ling, CHEN Zheng, LIU Bing, et al. Transition from metastability to instability in dynamics for the precipitation of $\delta'(Al_3Li)$ [J]. Rare Metals, 2001, 20(4): 240 ~ 247.

[8]　Chen L Q, Simmons J A. Microscopic master equation approach to diffusional transformations in inhomogeneous systems-single site approximation and direct exchange mechanism [J]. Acta Metall Mater, 1994, 42(9): 2943 ~ 2954.

[9]　ZHAO Yu-hong, CHEN Zheng, WANG Yong-xin, et al. Atomic-scale computer simulation for early precipitation process of $Ni_{75}Al_x V_{25-x}$ alloys with lower Al concentration [J]. The Chinese Journal of Nonferrous Metals, 2004, 14(3): 534 ~ 538. (in Chinese)

[10]　WANG Yong-xin, CHEN Zheng, LIU Bing, et al. Computer simulation on precipitation mechanism of phase in early stage in external energy field [J]. The Chinese Journal of Nonferrous Metals, 2004, 14(1): 255 ~ 262. (in Chinese)

[11]　Tomihisa K, Kaneno Y, Takasugi T. Phase relation and microstructure in multi-phase intermetallic alloys based on Ni_3Si-Ni_3Ti-Ni_3Nb pseudo-ternary alloy system [J]. Intermetallics, 2004, 12: 317 ~ 325.

[12]　Zapolsky H, Pareige C, Marteau L, et al. Atom probe analyses and numerical calculation of ternary phase diagram in Ni-Al-V system [J]. Calphad, 2001, 25(1): 125 ~ 134.

[13]　Pareige C, Blavette D. Simulation of the FCC $\rightarrow$ FCC+ $L1_2 + DO_{22}$ kinetic reaction [J]. Scripta Mater, 2001, 44: 243 ~ 247.

[14]　Poduri R, Chen L Q. Computer simulation of atomic ordering and compositional clustering in the pseudobinary Ni_3Al-Ni_3V system [J]. Acta Mater, 1998(46): 1719 ~ 1729.

[15]　Chen L Q. A computer simulation technique for spinodal decomposition and ordering in ternary systems [J]. Scripta Metallurgica et Materialia, 1993, 29: 683 ~ 688.

[16]　Lifshitz E M, Pitaevskii L P. Statistical Physics [M]. Oxford: Pergamon Press, 1980.

[17]　LI Xiao-ling, CHEN Zheng, LIU Bing. Computer studying of critical nucleus of ordered phase [J]. Nonferrous Metals, 2001, 53(3): 48 ~ 51. (in Chinese)

[18]　LI Xiao-ling. Atomic Scale Computer Simulation of Al_3Li Precipitation [D]. Xi'an: Northwestern Polytechnical University, 2002. (in Chinese)

[19]　Pareige C, Soisson F, Martin G. Ordering and phase separation in Ni-Cr-Al: Monte-Carlo simulation vs 3D atom probe [J]. Acta Mater, 1998, 47(6): 1889 ~ 1899.

[20]　Bendersky L K, Biancaniello F S, Williams M E. Solid-Solid Phase Transformation [M]. PA, Warrendale: TMS, 1994. 899 ~ 902.

(Edited by YANG Bing)